

FYS5419, project 1

Francesco Pogliano

April 2024

Abstract

In this report we introduce quantum computing and show how qubits are different from classical ones when it comes to the different values they may take, and the different gates one may apply to them. The variational quantum eigensolver (VQE) was also introduced, a hybrid quantum algorithm capable of finding the lowest energy eigenvalue of a Hamiltonian expressed in terms of the Pauli matrices. The VQE was used in order to first evaluate two toy models of 2×2 and 4×4 Hamiltonians, and then to evaluate the Lipkin model for two and four particles respectively. We see that the VQE manages to reproduce the results obtained with classical methods, and also outperform approximation schemes such as the Hartree-Fock. The choice of ansatz is though a central issue and given some focus especially for the $W = 0$ in the quasi-spin representation of the Lipkin Hamiltonian.

1 Introduction

Quantum computing is an emerging field of research that tries to take advantage of quantum mechanical properties of matter to improve certain aspects of computation that are difficult to achieve on classical computers. There are several differences between a quantum and a classical computer. One of them is the *qubit* replacing the classical bit. While bits only can take the values of 0 and 1, qubits are quantum-mechanical two-level systems that may take the values of 0, 1 and any superposition of these two states. The set of values a qubit may take is mapped on the surface of the Bloch sphere, and a good representation, familiar to anyone who has taken an introductory course in quantum mechanics, is the different spin states an electron (or any fermion of spin $1/2$) may take. Using the Dirac bra-ket notation, we may introduce the basis

$$|0\rangle = \begin{pmatrix} 1 \\ 0 \end{pmatrix}, \quad |1\rangle = \begin{pmatrix} 0 \\ 1 \end{pmatrix}, \quad (1)$$

where we have written their matrix notation equivalent on the side. Qubits live in quantum circuits. A quantum circuit consists of different qubits on which we can perform different operations in order to modify their state. These operations are called “gates”, and they correspond to quantum mechanical operators acting

on a two-state quantum system. The most used single-qubit quantum gates are the three Pauli matrices σ_x , σ_y and σ_z , the Phase gate P , and the Hadamard gate H . Their matrix representation is:

$$I = \begin{pmatrix} 1 & 0 \\ 0 & 1 \end{pmatrix}, \quad \sigma_x = \begin{pmatrix} 0 & 1 \\ 1 & 0 \end{pmatrix}, \quad \sigma_y = \begin{pmatrix} 0 & -i \\ i & 0 \end{pmatrix},$$

$$\sigma_z = \begin{pmatrix} 1 & 0 \\ 0 & -1 \end{pmatrix}, \quad P = \begin{pmatrix} 1 & 0 \\ 0 & i \end{pmatrix}, \quad H = \frac{1}{\sqrt{2}} \begin{pmatrix} 1 & 1 \\ 1 & -1 \end{pmatrix}$$

Where I is the identity matrix (no operation performed).

When acting on a basis state $|0\rangle$, we obtain:

$$I|0\rangle = \begin{pmatrix} 1 \\ 0 \end{pmatrix}, \quad \sigma_x|0\rangle = \begin{pmatrix} 0 \\ 1 \end{pmatrix}, \quad \sigma_y|0\rangle = \begin{pmatrix} 0 \\ i \end{pmatrix},$$

$$\sigma_z|0\rangle = \begin{pmatrix} 1 \\ 0 \end{pmatrix}, \quad P|0\rangle = \begin{pmatrix} 1 \\ 0 \end{pmatrix}, \quad H|0\rangle = \frac{1}{\sqrt{2}} \begin{pmatrix} 1 \\ 1 \end{pmatrix},$$

where we see how the gates transform the state. The identity, the phase gate and the σ_z gate leave the state unchanged. The reason for the first is obvious, while the second and the third represent a $\pi/2$ and π rotation around the z axis and leave the state unchanged ($|0\rangle$ is an eigenvector for σ_z). σ_x , or the NOT gate, represents a rotation around the x axis and flips the state to $|1\rangle$, while σ_y instead, representing a rotation around the y axis, achieves the same result as σ_x but with a different phase. Finally, the Hadamard gate puts the qubit into symmetric superposition. For the $|1\rangle$ basis state, we have instead

$$I|1\rangle = \begin{pmatrix} 0 \\ 1 \end{pmatrix}, \quad \sigma_x|1\rangle = \begin{pmatrix} 1 \\ 0 \end{pmatrix}, \quad \sigma_y|1\rangle = \begin{pmatrix} -i \\ 0 \end{pmatrix},$$

$$\sigma_z|1\rangle = \begin{pmatrix} 0 \\ -1 \end{pmatrix}, \quad P|1\rangle = \begin{pmatrix} 0 \\ i \end{pmatrix}, \quad H|1\rangle = \frac{1}{\sqrt{2}} \begin{pmatrix} 1 \\ -1 \end{pmatrix},$$

where only the identity matrix leaves the state unchanged. The σ_x gate flips it to $|1\rangle$, the σ_y also flips and adds a phase, P and the σ_z leave the state unchanged but add an i and a $i^2 = -1$ phase, and finally the Hadamard again puts the state in superposition, but in this case anti-symmetric.

On top of single-qubit gates, one also has multiple-qubit gates. The most important one is called CNOT gate, or Control-NOT gate. This gate entangles two qubits, and it performs a σ_x operation on the second qubit, if the first is found to be 1. This does not measure the qubit, meaning that the states are entangled: if for example the wavefunction is collapsed to $|0\rangle$ by measuring the first qubit, then a measurement on the second qubit will show that the value has been left unchanged, while a measurement of $|1\rangle$ on the first qubit will show that the second has been "flipped", or more correctly, that a σ_x gate has been enacted on it. The matrix representation of the CNOT gate is

$$\text{CNOT} = \begin{pmatrix} 1 & 0 & 0 & 0 \\ 0 & 1 & 0 & 0 \\ 0 & 0 & 0 & 1 \\ 0 & 0 & 1 & 0 \end{pmatrix}.$$

Bell states are defined as entangled states of two qubits. First, we may define a basis for a two-qubit system, as:

$$|00\rangle = |0\rangle_1 \otimes |0\rangle_2 = \begin{pmatrix} 1 \\ 0 \\ 0 \\ 0 \end{pmatrix}, \quad (2)$$

where $|0\rangle_1$ and $|0\rangle_2$ represent qubit 1 and 2 in state $|0\rangle$, and the Kroeneker product \otimes is the tensor product of the two basis vectors. Similarly, we can build the other three basis vectors as

$$|01\rangle = \begin{pmatrix} 0 \\ 1 \\ 0 \\ 0 \end{pmatrix}, |10\rangle = \begin{pmatrix} 0 \\ 0 \\ 1 \\ 0 \end{pmatrix}, |11\rangle = \begin{pmatrix} 0 \\ 0 \\ 0 \\ 1 \end{pmatrix}. \quad (3)$$

The four Bell states will then be defined as:

$$\begin{aligned} |\phi^+\rangle &= \frac{|00\rangle + |11\rangle}{\sqrt{2}} = \frac{1}{\sqrt{2}} \begin{pmatrix} 1 \\ 0 \\ 0 \\ 1 \end{pmatrix}, |\phi^-\rangle = \frac{|00\rangle - |11\rangle}{\sqrt{2}} = \frac{1}{\sqrt{2}} \begin{pmatrix} 1 \\ 0 \\ 0 \\ -1 \end{pmatrix} \\ |\psi^+\rangle &= \frac{|01\rangle + |10\rangle}{\sqrt{2}} = \frac{1}{\sqrt{2}} \begin{pmatrix} 0 \\ 1 \\ 1 \\ 0 \end{pmatrix}, |\psi^-\rangle = \frac{|01\rangle - |10\rangle}{\sqrt{2}} = \frac{1}{\sqrt{2}} \begin{pmatrix} 0 \\ 1 \\ -1 \\ 0 \end{pmatrix}. \end{aligned}$$

Bell states may be also created in a quantum circuit. The first thing to do would be to initialize the two qubits to state $|0\rangle$. Then a Hadamard gate is used on the first qubit, and a CNOT gate with qubit 2 as target is used on both qubits. The result will be a $|\phi^+\rangle$ state. When measuring Bell states (see

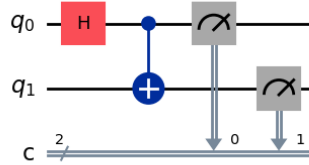


Figure 1: Circuit creating the Bell state ϕ^+ .

fig. 1), the measurement of the first qubit will inevitably decide the outfall of a measurement of the second qubit. In $|\phi^+\rangle$ for example, a measurement of 0 on

the first qubit, will necessarily give 0 on the second as well. This can be checked by simulating this quantum circuit. The code can be found in `part_a.py` in the Github repository, where functions are introduced and explained. Intuitively, when measuring one qubit in a 2-qubit circuit, we would like to first take a projection of the first qubit on, e.g. the $|0\rangle$ state, meaning filtering out all the information about the second qubit and calculating the probability of getting 0 after a measurement on it. Mathematically, we can use a projection operator $P_{0,2}$, where we indicate with 0 the index of the qubit we want to filter, and with 2 the dimension of the matrix:

$$P_{0,2} = P_0 \otimes I = \begin{pmatrix} 1 & 0 \\ 0 & 0 \end{pmatrix} \otimes \begin{pmatrix} 1 & 0 \\ 0 & 1 \end{pmatrix} = \begin{pmatrix} 1 & 0 & 0 & 0 \\ 0 & 1 & 0 & 0 \\ 0 & 0 & 0 & 0 \\ 0 & 0 & 0 & 0 \end{pmatrix},$$

and similarly for $P_{1,2}$. The probabilities of different measurements are encoded in the density matrix, defined as

$$\rho = |\psi\rangle \langle\psi|$$

for a general state $|\psi\rangle$. The probability of obtaining 0 after a measurement on the first qubit will be then given by the trace on the product of the projection operator and the density matrix:

$$\text{Tr}(P_{0,2}\rho).$$

In case of the Bell state $|\phi^+\rangle$, the result will give 0.5, as there is a 50% chance of measuring 0 after a measurement on the first qubit. After a measurement, the state collapses, and the result of a measurement on the second qubit is in principle certain. This can be simulated, and simulating this measurement 1000 times, yields 521 counts for $|00\rangle$, 479 for $|11\rangle$ and 0 for the remaining two. Similarly, using IBMs Qiskit[5], the results for 1000 shots is 515 for $|00\rangle$ and 485 for $|11\rangle$.

If we were to apply a Hadamard gate and a CNOT gate on a Bell state, meaning a circuit like the one in Fig. 2

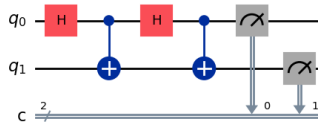


Figure 2: Bell state ϕ^+ with added Hadamard and CNOT gate.

The results for 1000 shots will be $|00\rangle = 258$, $|01\rangle = 252$, $|10\rangle = 241$ and $|11\rangle = 249$ counts, meaning a 25% change to obtain either result. Using Qiskit,

the results are similar, at 255, 256, 266 and 223. The results are somewhat surprising. Looking at the circuit, the first qubit, a part for being the subject of the control for the CNOT gate, it only experiences two Hadamard gates. These should cancel each other ($H^2 = I$) and one would not expect counts in states $|10\rangle$ and $|11\rangle$. The fact that this is not the case can be seen mathematically. The circuit can be expressed as

$$\begin{aligned} \text{CNOT}H_0\text{CNOT}H_0|00\rangle &= \text{CNOT}H_0|\phi^+\rangle \\ &= \begin{pmatrix} 1 & 0 & 0 & 0 \\ 0 & 1 & 0 & 0 \\ 0 & 0 & 0 & 1 \\ 0 & 0 & 1 & 0 \end{pmatrix} \frac{1}{\sqrt{2}} \begin{pmatrix} 1 & 0 & 1 & 0 \\ 0 & 1 & 0 & 1 \\ 1 & 0 & 1 & 0 \\ 0 & -1 & 0 & -1 \end{pmatrix} \frac{1}{\sqrt{2}} \begin{pmatrix} 1 \\ 0 \\ 0 \\ 1 \end{pmatrix} = \frac{1}{2} \begin{pmatrix} 1 \\ 1 \\ 1 \\ 1 \end{pmatrix}. \end{aligned}$$

This shows how the CNOT gate acts on two qubits at once, and that the controlled qubit is also affected by the operation.

In the following subsections we will explore how we can find the lowest eigenvalue for interacting Hamiltonians in a classical way, and using a quantum algorithm called variational quantum eigensolver (VQE).

1.1 Interacting Hamiltonian

In the following we will consider a 2×2 Hamiltonian $H = H_0 + \lambda H_I$, where

$$H_0 = \begin{pmatrix} E_1 & 0 \\ 0 & E_2 \end{pmatrix} \quad (4)$$

is the non interacting part, and

$$\begin{pmatrix} V_{11} & V_{12} \\ V_{21} & V_{22} \end{pmatrix} \quad (5)$$

is the interacting part. Here λ is the strength of the interaction. The Hamiltonian may be described in terms of the Pauli matrices in this way:

$$H_0 = \mathcal{E}I + \Omega\sigma_z, \quad H_I = cI + \omega_x\sigma_x + \omega_z\sigma_z, \quad (6)$$

where $\mathcal{E} = (E_1 + E_2)/2$, $\Omega = (E_1 - E_2)/2$, $c = (V_{11} + V_{22})/2$, $\omega_z = (V_{11} - V_{22})/2$ and $\omega_x = V_{12} = V_{21}$. The eigenvalues ϵ_0 and ϵ_1 can be found for the whole Hamiltonian H numerically, in the code `part_b.py`. In Fig. 3 (left) we observe how the eigenvalues evolve as a function of $\lambda \in [0, 1]$, and in Fig. 3 (right) how big is the overlap of $|0\rangle$ and $|1\rangle$ (the eigenvectors of the noninteracting Hamiltonian with eigenvalues E_1 and E_2) with the first eigenvector of H with eigenvalue ϵ_0 .

Here we see that at the λ threshold $\lambda_t = 2/3$ something interesting happens. While the eigenvector changes from being mostly dominated by the $|0\rangle$ component to being dominated by the $|1\rangle$ component at λ_t , the corresponding eigenvalue first increases, and then bends down. This behaviour is called "avoided crossing" and the energy level changes character from being symmetric at low λ s, to being anti-symmetric.

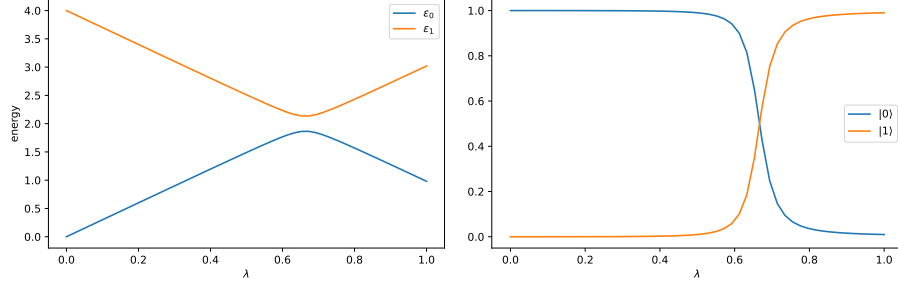


Figure 3: Eigenvalues (left) and the $|0\rangle$ and $|1\rangle$ components of the first eigenvector for the interacting Hamiltonian in Eq. (6).

1.2 The Variational Quantum Eigensolver

The variational quantum eigensolver (VQE) is a hybrid (classical plus quantum) algorithm with the aim to numerically evaluate the value of the lowest eigenvalue for a specific operator. In general terms, the algorithm first guesses a parametrised ansatz (e.g. a set of parametrised states), and runs them through the observable matrix (usually a Hamiltonian), calculates the result and the gradient with respect to the ansatz' parameters, and updates the ansatz with the new improved parameters. The eigenvalues are found when the ansatz correspond to the observable's eigenvectors. While the optimization part (gradient descent) is run on classical computers, the eigenvalue evaluation is carried out on a quantum computer. This last part is possible because the Pauli matrices (together with the identity matrix) create a basis for all 2×2 Hermitian matrices, and their Kroeneker products also may create a basis for all square Hermitian matrices. In this way we can always recast an observable (whose matrix must be Hermitian) as a linear combination of Pauli matrices. The expectation value of the observable will then be the sum of the expectation values of each term, which consists of a Pauli matrix and a coefficient. As an example, we may run a quantum circuit 1000 times, and if we measure 400 times the state $|1\rangle$, the expectation value for a σ_z measurement will be $400/1000 = 0.4$. Since quantum computers usually only can do measurements in the z basis, the expectation values along the other axes are done by first rotating (=applying quantum gates to) the qubits in such a way that the results of a measurement along the z axis would correspond to the result along the previous axis.

We try first the VQE on the Hamiltonian in Eq. (6), using IBM's Qiskit package. Qiskit is a powerful Python package that permits to simulate quantum circuits and algorithms, as well as sending jobs to real quantum computers. In this case, the VQE algorithm was run using an *estimator primitive*, a Qiskit tool where the expectation value of a circuit (in this case our Hamiltonian) is automatically calculated by running the circuit and measuring the output a certain number of times (shots). Since we only need one qubit, the ansatz will have two rotation gates, corresponding to the two angles mapping the Bloch

sphere. By tweaking these two angles, we will be able to find the Hamiltonian's eigenvectors.

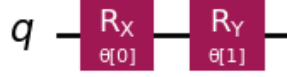


Figure 4: Ansatz for a 1-qubit circuit used for the VQE in part c.

The Qiskit VQE works well and it compares to the results from the classical evaluation, as we can see in Fig. 5. The code can be seen in `Part_c.py`.

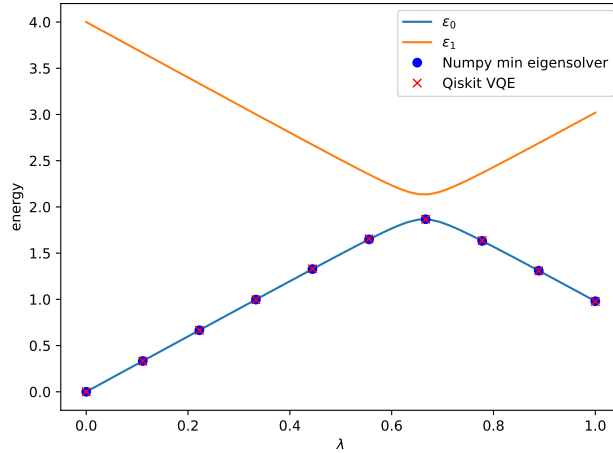


Figure 5: Lowest eigenvalue for the Hamiltonian in Eq. (6) calculated using VQE.

1.3 Two-qubits and entanglement

Until now we have analysed a one-qubit system, capable of representing a two-levels system described by a 2×2 Hamiltonian. When having two qubits, we can describe two, possibly coupled, two-level systems. In this case the Hamiltonian will be a 4×4 Hermitian matrix, which can be decomposed into $\sigma_i \otimes \sigma_j$, where σ_i, j may be any Pauli matrix or the 2×2 identity matrix. Given a Hamiltonian, we can use the same algorithms described before to calculate its eigenvalues, may it be numerically using linear algebra, or using quantum algorithms such as the

VQE. As an example, we introduce the 4×4 Hamiltonian:

$$H = H_0 + \lambda H_I = \begin{pmatrix} E_0 & 0 & 0 & 0 \\ 0 & E_1 & 0 & 0 \\ 0 & 0 & E_2 & 0 \\ 0 & 0 & 0 & E_3 \end{pmatrix} + \lambda \begin{pmatrix} H_z & 0 & 0 & H_x \\ 0 & -H_z & H_x & 0 \\ 0 & H_x & -H_z & 0 \\ H_x & 0 & 0 & H_z \end{pmatrix} \quad (7)$$

, where λ is as usual the strength of the interaction, and H_z and H_x are constants. We can easily see how E_0, E_1, E_2, E_3 are the eigenvalues of the non-interacting Hamiltonian H_0 , and its eigenvectors are the ones described in Eqs. (2) and (3). Using the same procedure as for the one-qubit case, we calculate and plot the eigenvalues in Fig. 8. Here we can see how the two lowest eigenvalues perform a level crossing at $\lambda \approx 0.4$, where the lowest eigenvalue bends sharply and continues downwards for increasing λ s. Another interesting quantity that can be measured with entangled systems, is the entanglement entropy. This quantity measures the quantity of entanglement between two subsystems. This is calculated as

$$S_A = -\text{Tr}(\rho_A \log_2(\rho_A)) \quad (8)$$

where Tr means taking the trace of a matrix (the sum of its diagonal terms), \log_2 is the base-two logarithm and ρ_A the reduced density matrix, defined as

$$\rho_A = \text{Tr}_B(\rho) = \langle 0|_B \rho |0\rangle_B + \langle 1|_B \rho |1\rangle_B \quad (9)$$

for a two-qubit system with subsystems A and B . The same expressions can be made for S_B by switching the labels. The entropy for the first qubit can be seen in Fig. 6, and we see that it increases steadily, until at $\lambda \approx 4$ the entropy does a large jump. This indicates that the entanglement increases as the strength of the interaction increases, and that especially the first qubit becomes much more entangled when the levels cross. The codes for this part can be found in `Part.d.py`.

The system may be solved with VQE in the same way as the 2×2 system. First, one has to recast the Hamiltonian in terms of Pauli matrices. While one can easily see that H_I can be expressed as

$$H_I = H_x \sigma_x \otimes \sigma_x + H_z \sigma_z \otimes \sigma_z, \quad (10)$$

the non-interacting Hamiltonian requires some work. As the tensor products of Pauli matrices represent a basis for all Hermitian 4×4 matrices, we know that a linear combination of them will be able to represent H_0 . After some calculations, I find that

$$\begin{pmatrix} 1 & 0 & 0 & 0 \\ 0 & 0 & 0 & 0 \\ 0 & 0 & 0 & 0 \\ 0 & 0 & 0 & 0 \end{pmatrix} = \frac{II + ZZ + IZ + ZI}{4}, \quad \begin{pmatrix} 0 & 0 & 0 & 0 \\ 0 & 1 & 0 & 0 \\ 0 & 0 & 0 & 0 \\ 0 & 0 & 0 & 0 \end{pmatrix} = \frac{II - ZZ - IZ + ZI}{4},$$

$$\begin{pmatrix} 0 & 0 & 0 & 0 \\ 0 & 0 & 0 & 0 \\ 0 & 0 & 1 & 0 \\ 0 & 0 & 0 & 0 \end{pmatrix} = \frac{II - ZZ + IZ - ZI}{4}, \quad \begin{pmatrix} 0 & 0 & 0 & 0 \\ 0 & 0 & 0 & 0 \\ 0 & 0 & 0 & 0 \\ 0 & 0 & 0 & 1 \end{pmatrix} = \frac{II + ZZ - IZ - ZI}{4},$$

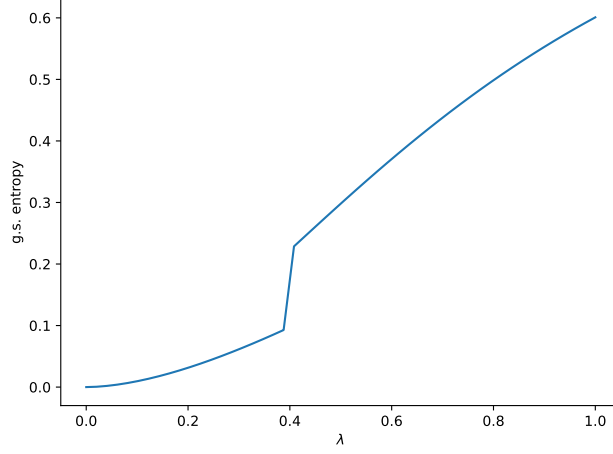


Figure 6: Entropy of the first qubit for the two-qubit Hamiltonian.

where II , ZZ etc. mean $I \otimes I$, $\sigma_z \otimes \sigma_z$ and so on. From this, one can rewrite the non-interacting Hamiltonian as

$$H_0 = \frac{E_0 + E_1 + E_2 + E_3}{4} II + \frac{E_0 - E_1 - E_2 + E_3}{4} ZZ + \frac{E_0 - E_1 + E_2 - E_3}{4} IZ + \frac{E_0 + E_1 - E_2 - E_3}{4} ZI. \quad (11)$$

Again, I use Qiskit to solve the problem, in an analogous way to the 2×2 case. The only differences being a larger number of iterations needed for convergence, and a modified ansatz, including a CNOT gate in order to add entanglement to the qubits, and repeating the rotations (with new independent parameters) after the entanglement. A circuit representation of the new ansatz can be seen in Fig. 7, and the results of the VQE are shown in Fig. 8.

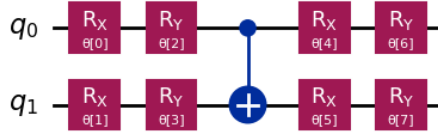


Figure 7: Ansatz for a 2-qubit circuit used for the VQE in part e.

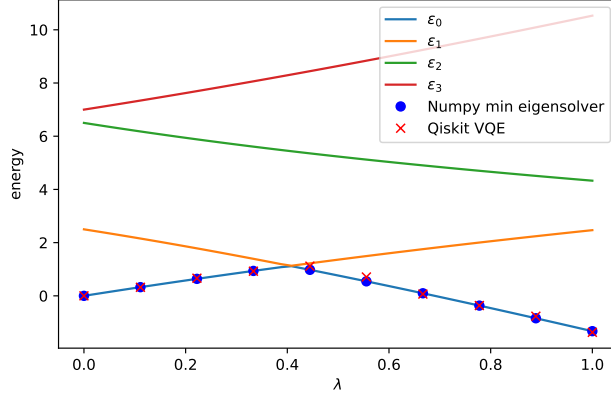


Figure 8: Eigenvalues for the 4×4 Hamiltonian in Eq. (7), with classical and Qiskit VQE results, using the ansatz of Fig. 7.

2 The Lipkin model

The Lipkin model, ideated in 1965 [1], is a model used to represent quantum many-body problems. The model can be used to describe the behaviour of 2 or more fermions in a two-level quantum system. For the case of four fermions, which will be the one we analyze here, we may think of the system as having two energy levels, each with degeneracy $d = 4$. The lower energy level with quantum number $\sigma = -1$ has energy $\varepsilon_1 = -\varepsilon/2$ and the upper level $\sigma = +1$ and $\varepsilon_2 = \varepsilon/2$ respectively. By characterizing the substates p , these can take the values $p = 1, 2, 3, 4$. From this, we may express the second-quantization Hamiltonian as

$$\begin{aligned}
 \hat{H} &= \hat{H}_0 + \hat{H}_1 + \hat{H}_2 \\
 \hat{H}_0 &= \frac{1}{2}\varepsilon \sum_{\sigma,p} \sigma a_{\sigma,p}^\dagger a_{\sigma,p} \\
 \hat{H}_1 &= \frac{1}{2}V \sum_{\sigma,p,p'} a_{\sigma,p}^\dagger a_{\sigma,p'}^\dagger a_{-\sigma,p'} a_{-\sigma,p} \\
 \hat{H}_2 &= \frac{1}{2}W \sum_{\sigma,p,p'} a_{\sigma,p}^\dagger a_{-\sigma,p'}^\dagger a_{\sigma,p'} a_{-\sigma,p}
 \end{aligned} \tag{12}$$

where $a_{\sigma,p}^\dagger$ and $a_{\sigma,p}$ are the creation and annihilation operators for a particle in the energy level σ in substate p , respectively, while V and W are constants.

This Hamiltonian can be rewritten in terms of the quasi-spin operators

$$\begin{aligned}
\hat{J}_+ &= \sum_p a_{p+}^\dagger a_{p-} \\
\hat{J}_- &= \sum_p a_{p-}^\dagger a_{p+} \\
\hat{J}_z &= \frac{1}{2} \sum_{p\sigma} \sigma a_{p\sigma}^\dagger a_{p\sigma} \\
\hat{J}^2 &= J_+ J_- + J_z^2 - J_z
\end{aligned} \tag{13}$$

as

$$\begin{aligned}
\hat{H} &= \hat{H}_0 + \hat{H}_1 + \hat{H}_2 \\
\hat{H}_0 &= \varepsilon J_z \\
\hat{H}_1 &= \frac{1}{2} V (J_+^2 + J_-^2) \\
\hat{H}_2 &= \frac{1}{2} W (-N + J_+ J_- + J_- J_+),
\end{aligned} \tag{14}$$

where $N = \sum_{p,\sigma} a_{p\sigma}^\dagger a_{p\sigma}$ is the number operator.

In this model, J is a good quantum number, and its J_\pm operators correspond to ladder operators, and obey the usual spin commutation relations. For four particles, this corresponds to a $J = 2$ system, where the five allowed states correspond to its J_z projections $J_z = -2, -1, 0, 1, 2$. Using the notation $|J, J_z\rangle$, for example $|2, -2\rangle$ would correspond to when all particles are in the lower level, $|2, -1\rangle$ with only one particle in the upper level, and so on until $|2, 2\rangle$ where all particles are in the upper level. The lifting operator then behaves like

$$J_+ |J, J_z\rangle = \sqrt{J(J+1) - J_z(J_z+1)} |J, J_z+1\rangle \tag{15}$$

and the lowering operator like

$$J_- |J, J_z\rangle = \sqrt{J(J+1) - J_z(J_z-1)} |J, J_z-1\rangle. \tag{16}$$

When constructing a Hamiltonian matrix, we will need to evaluate its matrix elements. Regardless of the number of particles and the value of J , we can find a general solution. We start by observing that the Hamiltonian will only have non-zero elements along the diagonal (handled by the H_0 and H_2 terms), and for those elements for which the difference between the z quasi-spin projections is $\Delta J_z = 2$ (handled by the H_1 term). Using the J_z and the lifting and lowering

operators, we can find a general expression for the diagonal terms.

$$\begin{aligned}
\langle J, J_z | H_0 + H_2 | J, J_z \rangle &= \varepsilon J_z + \frac{W}{2} (-N + J_+ J_- + J_- J_+) \\
&= \varepsilon J_z + \frac{W}{2} (-N + J_+ J_- + J_- J_+) \\
&= \varepsilon J_z + \frac{W}{2} (-N + 2J(J+1) - J_z(J_z - 1) - J_z(J_z + 1)) \\
&= \varepsilon J_z + \frac{W}{2} (-N + 2J(J+1) - 2J_z^2) \\
&= \varepsilon J_z + W \left(-\frac{N}{2} + J(J+1) - J_z^2 \right),
\end{aligned}$$

and since we are talking of fermions, we may also simplify $N = 2J$, and obtain

$$\langle J, J_z | H_0 + H_2 | J, J_z \rangle = \varepsilon J_z + W (J^2 - J_z^2). \quad (17)$$

The non-diagonal, non-zero terms instead have a more complicated expression, but can still be extracted from the ladder operators:

$$\begin{aligned}
\langle J, J_z \pm 2 | H_1 | J, J_z \rangle &= \langle J, J_z | H_1 | J, J_z \pm 2 \rangle = \\
&= \frac{V}{2} [(J(J+1) - J_z(J_z \pm 1)) \times (J(J+1) - (J_z \pm 1)(J_z \pm 2))]^{1/2}. \quad (18)
\end{aligned}$$

In order to solve this problem on a quantum computer, we need to recast the Hamiltonian in terms of identity and Pauli matrices. Following the lecture notes, This can be done by choosing a mapping scheme, in this case imagining every two-level doublet as a qubit, where the lower level is represented by the state $|1\rangle$ and the excited level by the state $|0\rangle$. In other words, the two-particle system will be represented by two qubits, each for every particle. To translate the two-particle Hamiltonian to Pauli matrices, we first notice how we can translate the J operators into single-particle operators:

$$J_\sigma = \sum_n j_\sigma^{(n)}, \quad J_\pm = \sum_n j_\pm^{(n)}, \quad j_\pm^{(n)} = j_x^{(n)} \pm i j_y^{(n)} \quad (19)$$

for $n, m < N$ where N is the number of particles we have in the system. Using these expressions, our Hamiltonian becomes

$$\begin{aligned}
H &= \varepsilon \sum_n j_z^{(n)} + \frac{1}{2} V \sum_{n \neq m}^N \left(j_+^{(n)} j_+^{(m)} + j_-^{(n)} j_-^{(m)} \right) + \frac{1}{2} W \sum_{n \neq m}^N \left(j_+^{(n)} j_-^{(m)} + j_-^{(n)} j_+^{(m)} \right) \\
&= \varepsilon \sum_n j_z^{(n)} + V \sum_{n \neq m}^N \left(j_x^{(n)} j_x^{(m)} - j_y^{(n)} j_y^{(m)} \right) + W \sum_{n \neq m}^N \left(j_x^{(n)} j_x^{(m)} + j_y^{(n)} j_y^{(m)} \right), \quad (20)
\end{aligned}$$

where $n \neq m$ because acting twice on the same particle would throw it below the ground level, or above the first (and only) excited level¹. One may obtain the same expression in the lecture notes if one observes that n and m may be swapped and give the same result, and only consider the terms where $n < m$, and multiplying the V term by two. Finally, we substitute $j_x^{(n)} = X_{(n)}/2$ where X is the σ_x Pauli matrix (and similarly for Y and Z), and the factor of two is in order to account for the fact that spins give $\pm 1/2$ eigenvalues, while Pauli matrices give ± 1 . Finally, our general Hamiltonian case looks like

$$H = \frac{\varepsilon}{2} \sum_n Z_n + \frac{V}{2} \sum_{n \neq m} (X_n X_m - Y_n Y_m) + \frac{W}{2} \sum_{n \neq m} (X_n X_m + Y_n Y_m), \quad (21)$$

where with Z_n we mean $I_1 \otimes I_2 \otimes \dots \otimes Z_n \otimes \dots \otimes I_N$ and with $A_n B_m$ we mean $I_1 \otimes I_2 \otimes \dots \otimes A_n \otimes \dots \otimes B_m \otimes \dots \otimes I_N$.

2.1 $J = 1$, two particles

We start analyzing the problem by just having two particles. In the case of two particles, the problem simplifies to $J = 1$, where $|1, -1\rangle$ corresponds to both particles in the lower level, $|1, 0\rangle$ with one particle down and one up, and finally $|1, 1\rangle$ with both particles up. We may construct the matrix using our simplified $|J = 1, J_z\rangle$ basis using the expressions from Eqs. (17) and (18), obtaining

$$\begin{pmatrix} -\varepsilon & 0 & V \\ 0 & W & 0 \\ V & 0 & \varepsilon \end{pmatrix}. \quad (22)$$

The Hamiltonian in Eq. (22) is easily diagonalised by finding the roots of the characteristic polynomial

$$\det \begin{pmatrix} -\varepsilon - \lambda & 0 & V \\ 0 & W - \lambda & 0 \\ V & 0 & \varepsilon - \lambda \end{pmatrix}, \quad (23)$$

which gives

$$H = \begin{pmatrix} \sqrt{\varepsilon^2 + V^2} & 0 & 0 \\ 0 & W & 0 \\ 0 & 0 & -\sqrt{\varepsilon^2 + V^2} \end{pmatrix}. \quad (24)$$

The plots in Fig. 9 show the three eigenvalues as V changes from 0 to 2, for two values of W .

We can recast this matrix in a way that is solvable by quantum computers, i.e. in terms of Pauli matrices. We use the expressions in Eq. (21) and obtain

$$H = \frac{\varepsilon}{2} (ZI + IZ) + \frac{V}{2} (XX - YY) + \frac{W}{2} (XX + YY). \quad (25)$$

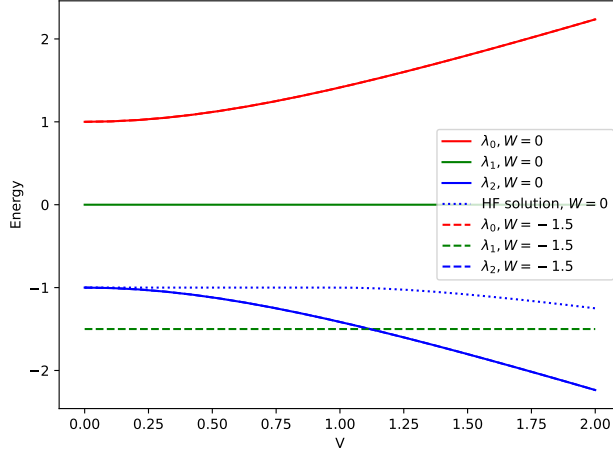


Figure 9: Eigenvalues for the 4×4 Hamiltonian in Eq. (7) for two different values of W . Since only the central eigenvalue of the Hamiltonian depends on W , the two other eigenvalues overlap. Hartree-Fock solution plotted for comparison.

The VQE solution can be seen in Fig. 10 (code `part_fg3x3.py`).

Here we see that the VQE does generally a good work in guessing the lowest eigenvalue even in the occurrence of level crossing, with only some few mistakes around the crossing that might be mitigated with more iterations of the VQE algorithm.

2.1.1 The $W = 0$ case

For $W = 0$ we can exploit the symmetries of the Hamiltonian and reduce it to a 2×2 matrix using the Grey code encoding scheme[2, 3], as used in Ref. [4]. We then obtain the Hamiltonian

$$H = \begin{pmatrix} E & V \\ V & -E \end{pmatrix} = EZ + VX, \quad (26)$$

where we already have recasted it in terms of Pauli matrices on the right hand side. This Hamiltonian may be solved with only one qubit in a similar way as the first problem we solved. According to Ref. [4], this Hamiltonian only needs an ansatz consisting of a $R_y(\theta)$ gate with one parameter θ , and we observe that it converges quite quickly and precisely (see Fig. 11, pointing to the importance of casting the problem into a more manageable one for quantum computers.

¹Mathematically, this is an unnecessary specification, as the ladder operators already take care of this by yielding a factor of zero if one tries to annihilate the ground state, or excite the most excited state.

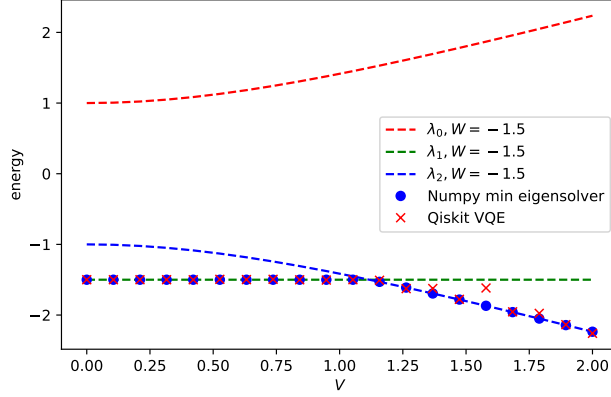


Figure 10: Eigenvalues for the 4×4 Hamiltonian in Eq. (25) for $W = -1.5$, with classical and Qiskit VQE results, using the ansatz of Fig. 7.

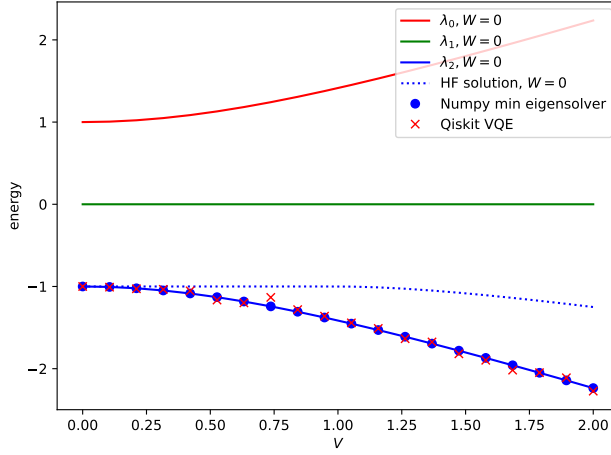


Figure 11: Eigenvalues for the 4×4 Hamiltonian in Eq. (26), and VQE results.

2.2 $J = 2$, four particles

The 4-particle case is an expansion of the 2-particle model, where in the computational basis we have five different configurations. The quasi-spin will be $J = 2$, and the configurations will run from $|2, -2\rangle$ where all the particles are in their ground state, to $|2, 2\rangle$ where they are all excited to their top excited level. The same general Hamiltonian as in Eq. (14) may be used and we may calculate the Hamiltonian's nonzero matrix elements again using the expressions in Eqs. (17)

and (18)

$$H = \begin{pmatrix} -2\varepsilon & 0 & \sqrt{6}V & 0 & 0 \\ 0 & -\varepsilon + 3W & 0 & 3V & 0 \\ \sqrt{6}V & 0 & 4W & 0 & \sqrt{6}V \\ 0 & 3V & 0 & \varepsilon + 3W & 0 \\ 0 & 0 & \sqrt{6}V & 0 & 2\varepsilon \end{pmatrix}. \quad (27)$$

This Hamiltonian is harder to diagonalize as the characteristic polynomial is of the fifth order, so a numerical solution is presented in `Part_fg5x5.py` and in Fig. 12.

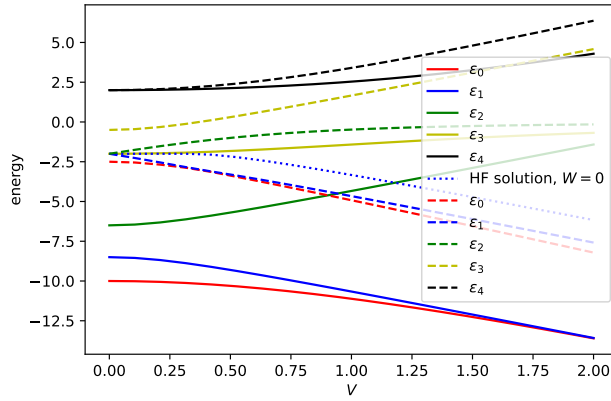


Figure 12: Eigenvalues for the 5×5 Hamiltonian in Eq. (27) for two different values of W .

In order to solve this by VQE, it will have to be expressed in terms of Pauli matrices. Since we have four particles, we will need four qubits, and thus a 16×16 matrix. We may still use the expression in Eq. (21), and obtain

$$H = \frac{\varepsilon}{2} \sum_n Z_n + \frac{V}{2} \sum_{n \neq m} (X_n X_m - Y_n Y_m) + \frac{W}{2} \sum_{n \neq m} (X_n X_m + Y_n Y_m), \quad (28)$$

resulting in

$$\begin{aligned} H = & \frac{\varepsilon}{2} (ZIII + IZII + IIZI + IIIZ) \\ & + \frac{W+V}{2} (XXII + XIXI + XII X + IXXI + IXIX + IIXX) \\ & + \frac{W-V}{2} (YYII + YIYI + YIIY + IYYI + IYIY + IYY Y). \end{aligned} \quad (29)$$

The VQE for $W \neq 0$ is hard to compute, and even for many iterations the VQE struggles to converge to the classical results. Nevertheless the results are in the right ballpark, as can be seen in Fig. 13, for $W = -0.5$. The ansatz used

is shown in Fig. 14. Three repetitions of the Qiskit TwoLocal rotation ansatz were needed for convergence.

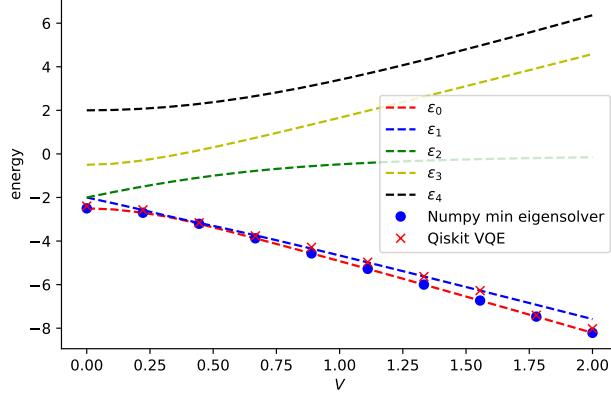
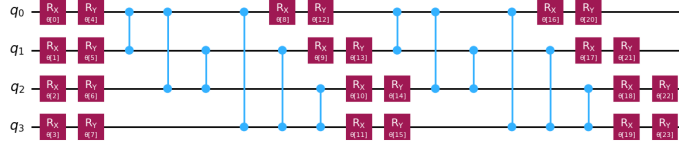


Figure 13: Eigenvalues for the 5×5 Hamiltonian in Eq. (29) for $W = 0$, plus the VQE solution, using the ansatz of Fig. 14.



We may then use the VQE using the ansatz proposed by Ref. [4] (Fig. 15 consisting of only two qubits, a R_y and a control R_y gates and only two parameters. The convergence is much more rapid and precise, and shown in Fig. ??

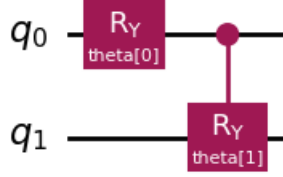


Figure 15: Ansatz used for the VQE evaluation of the Hamiltonian in Eq. (31).

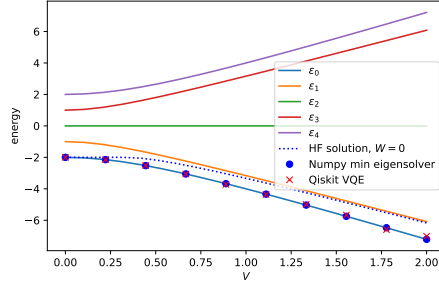


Figure 16: Eigenvalues for the simplified 4×4 Hamiltonian in Eq. (31), using the ansatz in Fig. 15.

3 Conclusion

In this report we have introduced quantum computing and its general components, such as qubits, quantum gates and the interpretation of outputs as expectation values of the Z spin operator. We have also introduced the variational quantum eigensolver (VQE), an hybrid algorithm capable of finding the lowest energy eigenvalue of a Hamiltonian expressed in terms of the Pauli matrices. This algorithm requires a parametrized ansatz (which can be interpreted as a trial wavefunction) which is run on the quantum computer to obtain an expectation value, for then minimizing the parameters via gradient descent. The VQE was first tested on two toy models of one and two qubits, and then tested on the Lipkin model for two and four particles. We see that the VQE manages to reproduce the results obtained with classical methods, and also outperform

approximation schemes such as the Hartree-Fock. The choice of ansatz is though a central issue, important not only for shorter computation times, but also the feasibility of the minimization problem. We see that the Hamiltonian should be simplified when possible to be modeled with as few qubits and gates as possible, to reduce noise and increase feasibility on current-state, noisy quantum computers. Especially, symmetries arising from simplification schemes (e.g. when $W = 0$) should be properly exploited to achieve better precision.

References

- [1] H.J. Lipkin, N. Meshkov, and A.J. Glick. “Validity of many-body approximation methods for a solvable model: (I). Exact solutions and perturbation theory”. In: *Nuclear Physics* 62.2 (1965), pp. 188–198. ISSN: 0029-5582. DOI: [https://doi.org/10.1016/0029-5582\(65\)90862-X](https://doi.org/10.1016/0029-5582(65)90862-X). URL: <https://www.sciencedirect.com/science/article/pii/002955826590862X>.
- [2] Nicolas P. D. Sawaya et al. “Resource-efficient digital quantum simulation of d-level systems for photonic, vibrational, and spin-s Hamiltonians”. In: *npj Quantum Information* 6.1 (June 2020), p. 49. ISSN: 2056-6387. DOI: 10.1038/s41534-020-0278-0. URL: <https://doi.org/10.1038/s41534-020-0278-0>.
- [3] Nicolas P. D. Sawaya et al. “Resource-efficient digital quantum simulation of d-level systems for photonic, vibrational, and spin-s Hamiltonians”. In: *npj Quantum Information* 6.1 (June 2020), p. 49. ISSN: 2056-6387. DOI: 10.1038/s41534-020-0278-0. URL: <https://doi.org/10.1038/s41534-020-0278-0>.
- [4] Manqoba Q. Hlatshwayo et al. “Simulating excited states of the Lipkin model on a quantum computer”. In: *Phys. Rev. C* 106 (2 Aug. 2022), p. 024319. DOI: 10.1103/PhysRevC.106.024319. URL: <https://link.aps.org/doi/10.1103/PhysRevC.106.024319>.
- [5] Qiskit contributors. *Qiskit: An Open-source Framework for Quantum Computing*. 2023. DOI: 10.5281/zenodo.2573505.